Chapter 4

Force Measurements between Activated Silica Surfaces in Sodium Oleate Solutions

4.1 Introduction

Hydrophobic forces were first observed by Israelachvili and Pashley (1) between two curved mica surfaces in 2.5×10^{-5}M cetyltrimethylammonium bromide (CTAB) solution. Since mica surfaces are negatively charged, cationic surfactants adsorbed on the surface and hydrophobized it. The measured hydrophobic force (F_h) were fit using the following expression:

$$F_h/R = -C_o \exp(-H/D_o) \quad (1)$$

where R is the radius of the mica cylinders used for the measurement, D_o=1.2 nm and C_o=30 mN/m. Hydrophobic forces have also been observed with other cationic surfactants, such as dodecylammoniumhydrochloride (DAHCl), octadecyl-ammoniumhydrochloride (OAHCl) and dihexadecyl-dimethyl ammonium acetate (DHDAA), in equilibrium with mica and silica surfaces (2,3). The C_o and D_o values obtained with these surfactants are comparable to those obtained with CTAB.

Pugh and Rutland (4) conducted force measurements with mica surfaces in equilibrium with an anionic surfactant, sodium laurate, at pH 10.3. They added Ca^{2+} ions to the solution to reverse the surface charge of the mica, which is referred to as 'activation' in flotation literature. However, the authors failed to detect any hydrophobic force, indicating that the anionic surfactant did not adsorb on the activated mica surface.

Hydrolizable cations are commonly used as activators for the adsorption of anionic

surfactants. For example, Ca^{2+} ions are added to activate anatase (TiO_2) during the process of separating this mineral from kaolin clay by flotation using fatty acids. Fuerstenau *et al*. (5) measured the ζ-potentials of silica and alumina in the presence of various hydrolizable cations. They found that with a given activator, ζ-potentials are reversed at a pH where the concentration of the singly charged hydroxo-complexes, $M(OH)_{(z-1)}^{+}$, becomes appreciable in solution. They also conducted microflotation tests with silica in the presence of alkyl sulfonate (6) using various hydrolizable cations (Fe^{3+}, Pb^{2+} and Mn^{2+}), and found that the flotation is most favored at the pH of maximum concentration of the singly charged hydroxo-complexes. Fuerstenau and Cummins (7) reported similar results for the flotation of quartz with sodium oleate in the presence of $CaCl_2$.

To explain the effectiveness of the singly-charged hydroxo-complexes as activator, Palmer *et al*. (8) suggested two possible mechanisms: i) hydroxo complexes are hydrogen bonded to the surface hydroxyl groups:

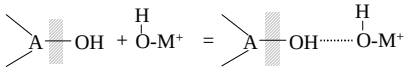

(2)

where A is the metal ion in the substrate and M is the hydrolizable cation, and ii) hydroxo-complexes chemisorb on the surface as follows:

$$A\text{-}OH + MOH^{+} = A\text{-}OM^{+} + H_2O. \qquad (3)$$

Both of these mechanisms suggest that the adsorption should give rise to large negative free energies of adsorption (ΔG^{o}_{ads}), which may provide an explanation for the experimental observation that singly charged hydroxo-complexes have higher adsorbability than the unhydrolyzed cations (M^{Z+}).

It should be noted here that while the mechanisms proposed by Palmer *et al*. (8) explains why the adsorption of the singly charged hydroxo-complexes should be favored, they do not explain why the unhydrolized cations do not adsorb on negatively charged surfaces. For the latter, James and Healy (9) subdivided ΔG^{o}_{ads} into three components:

$$\Delta G^{o}_{ads} = \Delta G^{o}_{elec} + \Delta G^{o}_{solv} + \Delta G^{o}_{chem} \quad (4)$$

where ΔG^{o}_{elec} represents the component from coulombic attraction, ΔG^{o}_{solv} represents the unfavorable free energy changes associated with the removal of the water molecules from secondary hydration sheath during the adsorption process, and ΔG^{o}_{chem} represents the component due to specific chemical interactions such as Reaction (3) above. They suggested that the ΔG^{o}_{solv} of the unhydrolized cations is much larger than that of the singly charged hydroxo-complexes. As a result, ΔG^{o}_{ads} of the former is more unfavorable than that of the latter. Indeed, it is well known that ΔG^{o}_{solv} decreases quadratically with charge (9). By calculating all three of the free energy component in Eq.(4), James and Healy were able to explain why unhydrolized cations cannot adsorb on silica. However, they assumed the same values of ΔG^{o}_{chem} for both the unhydrolyzed cations and the singly charged hydroxo-complexes. Also, the values of ΔG^{o}_{elec} were calculated using the values of surface potentials calculated from the Nernst equation, which are nearly an order of magnitude higher than those obtained from surface force measurements.

Schindler *et al*. (10) developed a completely different model, in which unhydrolized metal ions chemisorb on silica via an exchange mechanism involving the protons of the silanol groups. They simply assigned different equilibrium constants for the adsorption isotherms of various cations (i.e., Fe^{3+}, Pb^{2+}, Al^{3+} and Cu^{2+}). Their model does not provide a mechanistic explanation for the fact that the adsorption is a maximum at the pH where the singly charged hydroxo-complexes is maximum.

In the present communication, an atomic force microscope (AFM) was used to measure the surface forces between two silica surfaces in $MgCl_2$ and $CaCl_2$ solutions. The adsorption of these cations should not only change repulsive double-layer forces, but also hydration forces. It was shown previously that silica surfaces exhibit hydration forces in pure water (11-19), that diminishes in the presence of cations (14-18) and short-chain alcohols (13). The surface force measurements were also conducted between activated silica surfaces in the presence of sodium oleate. It is of particular interest to see if hydrophobic forces are observed under conditions of

maximum adsorption of oleate, which in turn may be related to the optimum conditions for activation.

4.2 Experimental

4.2a *Sample Preparation*

Optically smooth fused silica plates were obtained from Haraeus Amersil, Inc. They were cleaned by boiling in a nitric acid solution for 12 to 15 hours, and then equilibrated in conductivity water from a Barnstead Nanopure II water treatment unit. The clean silica plates thus obtained exhibited equilibrium contact angles (θ_{eq}) of less than 5^{o}, as measured using a Rame-Hart Model 100 goniometer. Glass spheres of radius 10 to 30 μm from Duke Scientific were mounted on cantilever tips by means of an adhesive (Epon R Resin 1004, Shell Chemical Company) (19,20), placed in NaOH solutions (pH~10) overnight, and equilibrated in Nanopure water before each experiment. Reagent grade $CaCl_2$ and $MgCl_2$ (both 99.3% purity) were obtained from Fischer Scientific. Purified sodium oleate from Fischer Scientific was used as received. A $2x10^{-3}$ M stock solution of oleate was prepared in 50% ethanol solution. Since the concentration of oleate used in the experiments was $1x10^{-4}$ M, the ethanol content never exceeded 2.5%.

4.2b *Methods and Apparatus*

A Digital Instruments Nanoscope III AFM was used to measure the forces between a silica plate and a glass sphere mounted at the tip of a cantilever. Both standard triangular silicon nitride and TESP were obtained from Digital Instruments Co. The stiffness of the cantilevers was measured by the technique of Senden and Ducker (19). This consists of placing a heavy tungsten sphere on the cantilever tip, turning the cantilever upside down and measuring its deflection from the AFM signal. The glass spheres were mounted on the cantilever using a micromanipulator. The mounted spheres, equilibrated in NaOH solutions and Nanopure water as described in the foregoing last section, were then transferred to a fluid cell for force measurements. The force measurements were conducted in Nanopure water and in solutions containing known

concentrations of $CaCl_2$ (or $MgCl_2$) and oleate. The surfaces were equilibrated for 15 minutes in each solution prior to the force measurements. The pH was adjusted by NaOH and measured be means of a glass electrode. The radius of the glass spheres was measured using a Kontron SEM-IPS image processing system.

4.3 Results

4.3a *Force Measurements with $MgCl_2$ and Oleate*

Figure 4.1 shows the effect of pH on the equilibrium contact angles (θ_{eq}) of silica plates in the presence of $2x10^{-4}$ M $MgCl_2$ and 10^{-4} M sodium oleate. The dotted lines represent the concentrations of the various Mg-species present in solution at $2x10^{-4}$ M $MgCl_2$. The thermodynamic data used for the calculations were taken from reference 21. As shown in the figure, θ_{eq} exhibits a maximum value of 70^o in the pH range of 11.0-11.3. At pH<11.0 and pH>12.0, the silica surface remains hydrophilic with θ_{eq}~5^o. One can see that the changes in θ_{eq} with pH correspond to the same in the concentration of the $Mg(OH)^+$ ion, suggesting that silica is activated by the singly charged hydroxo-complexes, rather than the Mg^+ ions, and that oleate adsorption is closely related to the activation mechanism. These findings are in agreement with the results of Fuerstenau *et al.* (6), who showed that the flotation of quartz is maximum at pHs where the concentrations of singly-charged hydroxo complexes are maximum.

Figure 4.2 shows the results of the direct surface force measurements conducted between glass sphere and silica plate using an AFM. The measurements were conducted i) in Nanopure water, ii) in solutions containing $2x10^{-4}$ M $MgCl_2$, and iii) in solutions containing the same amount of $MgCl_2$ and 10^{-4}M oleate. All the measurements were conducted at pH 5.7. The measured forces, F, normalized by the radius of the sphere, R, are plotted as a function of the separation distance, H. The dashed lines represent the constant charge model of the DLVO theory (19,20) fitted to the experimental data. The DLVO curves were obtained using the algorithm of Chan *et al*. (21). Force data obtained in Nanopure water can be fitted to the constant charge model of the DLVO theory using surface potential (ψ_o) of -57 mV, Debye length (κ^{-1}) of 96 nm, and the

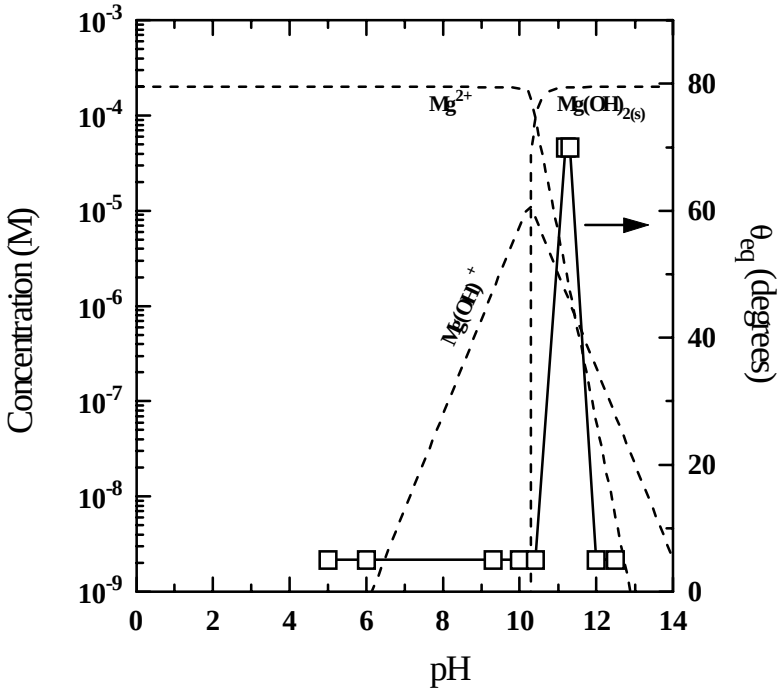

Figure 4.1. θ_{eq} vs pH (□) curve for a silica plate immersed in $2x10^{-4}$ M $MgCl_2$ and 10^{-4} M Na-Oleate. The dotted lines represent the concentrations of the various species present in solution.

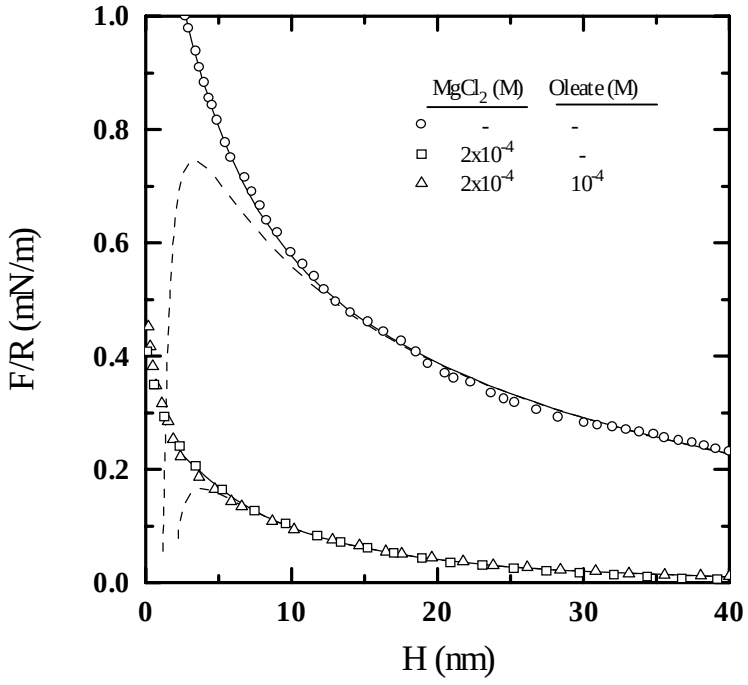

Figure 4.2. F/R vs H curves obtained between silica plate and glass sphere in i) Nanopure water (○), ii) $2x10^{-4}$ M $MgCl_2$ (□), and iii) $2x10^{-4}$ M $MgCl_2$ and 10^{-4} M sodium oleate (Δ) at pH 5.7. The dashed lines represent the constant charge model of the DLVO theory fitted to the data using the parameters listed in Table I. The solid lines represent the extended DLVO theory (Eq. [5]), incorporating a hydration force term.

.

Hamaker constant (A_{131}) of 6.3×10^{-21} J. These values are close to those reported previously (19).

At H<12 nm, the force curve obtained in Nanopure water shows repulsive forces larger than those predicted by the DLVO theory. This extraneous force, which has also been observed previously (22-24), is generally referred to as the hydration force. Therefore, the force data are fitted to the extended DLVO theory:

$$F_t = F_e + F_d + F_{hyd} \tag{5}$$

which includes contributions from the hydration force (F_{hyd}) in addition to those from the electrostatic (F_e) and dispersion (F_d) forces considered in the DLVO theory. The hydration force is represented by the following expression:

$$F/R = C_1 \exp(-H/D_1) + C_2 \exp(-H/D_2) , \tag{6}$$

where C_1=7.7 mJ/m^2, D_1=0.50 nm, C_2=0.50 mJ/m^2, and D_2=2.70 nm. These values are close to those estimated by Yoon and Yotsumoto (15) based on turbidity measurements.

Note in Figure 4.2 that the force data obtained in 2×10^{-4} M $MgCl_2$ can be fitted with ψ_o=-14 mV, which is much lower than ψ_o=-57 mV obtained in Nanopure water (Table 4.1). At 2×10^{-4} M $MgCl_2$, the theoretically calculated double layer thickness (κ^{-1}) is 11.0 nm. This value is comparable to that obtained by fitting the force data, which is 13.4 nm. The changes in ψ_o from –57 mV to –14 can be attributed to the double-layer compression rather than the neutralization of the negative charge sites by the adsorption of Mg^{2+} ions. This can be seen from the following approximate expression:

$$\psi_o = \sigma \kappa^{-1} / \varepsilon \varepsilon_0 \tag{7}$$

where σ is the surface charge, ε is the permitivitty of free space and ε_o the relative dielectric constant for water. It can be seen from Eq.[7] that if κ^{-1} decreases, ψ_o should also reduce.

Table 4.1

The Contact Angle and Surface Force Data obtained with silica in the presence of $MgCl_2$ and Na-Oleate at different pHs

pH	$MgCl_2$ (M)	Oleate (M)	θ_{eq}	ψ_0 (mV)	κ^{-1} (nm)	C_1 (mJ/m^2)	D_1 (nm)	C_2 (mJ/m^2)	D_2 (nm)
5.7	-	-	$<5^0$	-57	96.0	7.7	0.50	0.50	2.7
5.7	$2x10^{-4}$	-	$<5^o$	-14	13.4	8.0	0.46	0.40	1.4
5.7	$2x10^{-4}$	10^{-4}	$<5^o$	-14	13.4	8.0	0.46	0.40	1.4
11.2	-	-	$<5^o$	-30	11.0	7.0	0.41	0.40	0.8
11.2	$2x10^{-4}$	-	$<5^o$	0	-	-	-	-	-
11.2	$2x10^{-4}$	10^{-4}	70^o	+42	11.0	-30.0	2.10	-	-
12.0	-	-	$<5^o$	-12	3.5	8.0	0.42	-	-
12.0	$2x10^{-4}$	-	$<5^o$	-12	3.5	8.0	0.42	-	-
12.0	$2x10^{-4}$	10^{-4}	$<5^o$	-12	3.5	8.0	0.42	-	-

Therefore, decrease in ψ_o at $2x10^{-4}$M $MgCl_2$ should be attributed to double-layer compression.

It is interesting that in the presence of $2x10^{-4}$ M $MgCl_2$, the hydration force is still visible at H<5 nm, which further suggests that Mg^{2+} ions do not adsorb on silica at pH 5.7. Eq. [5] can be used to fit the hydration force using the parameters shown in Table I. As shown, D_2 is reduced by ~54% in the presence of $2x10^{-4}$M $MgCl_2$. It is well documented that the primary hydration force observed between silica surfaces decreases in the presence of cations (14-18).

Figure 4.2 shows that the force data obtained in solutions containing $2x10^{-4}$M $MgCl_2$ and 10^{-4} M oleate fall on the same curve as those obtained at $2x10^{-4}$ M $MgCl_2$ in the absence of oleate. As seen in Table I, there are no changes in the values of ψ_o and D_2 that were used for the fit the data. One can conclude, therefore, that oleate does not adsorb on silica at this pH 5.7. This finding is in agreement with the fact that, at these conditions, θ_{eq} remains in the neighborhood of ~5°.

Figure 4.3 shows the results of the AFM force measurements conducted between the glass sphere and silica plate at pH 11.2. In the absence of $MgCl_2$ and oleate, the experimental data obtained at H>5nm can be fitted to the DLVO theory with ψ_o=-30 mV. On the other hand, the data obtained at H<5 nm can only be fitted to the extended DLVO theory, which includes contributions from the hydration force. The data obtained in the absence of $MgCl_2$ and oleate have been fitted using the parameters listed in Table I. Note that both $-\psi_o$ and D_2 are lower than those obtained at pH 5.7, which may be attributed to the Na^+ ions introduced as NaOH for pH adjustment. At pH 11.2, the theoretically expected value of κ^{-1} is 7.5 nm, which is comparable to the value of 7.6 nm obtained by fitting the data to the DLVO theory.

Figure 4.3 also shows the results of force measurements conducted in a $2x10^{-4}$ M $MgCl_2$ solution at pH 11.2. No double layer repulsion is observed, suggesting that the charges on the silica surfaces have been neutralized. At H<10 nm, the forces are net attractive and the two surfaces jump into contact from a distance of 7 nm. The experimental data can be fitted to the van der Waals force alone with $A_{131}=6x10^{-21}$ J, as shown by the dashed line. The value of A_{131}

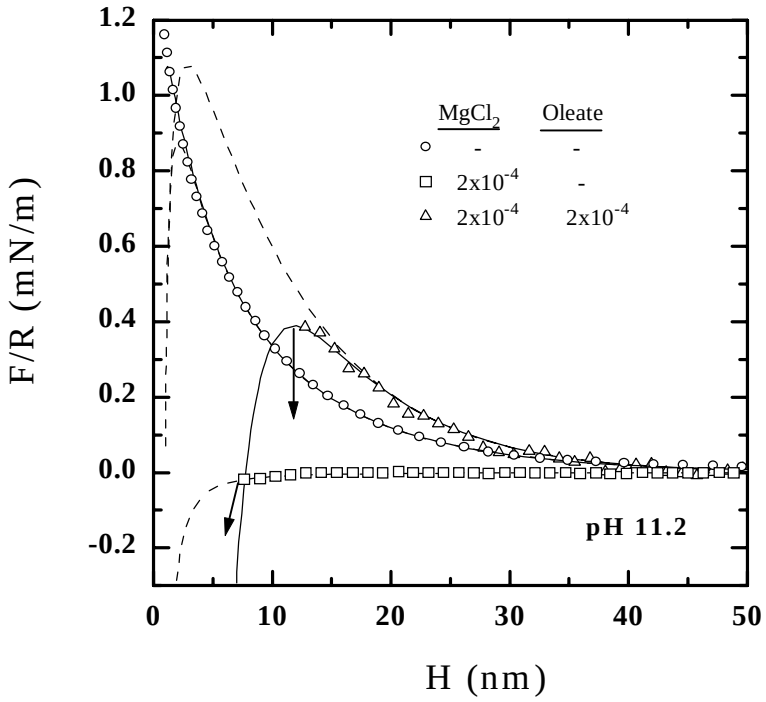

Figure 4.3. F/R vs H curves obtained between silica plate and glass sphere at pH 11.2 i) in the absence of $MgCl_2$ and sodium oleate (○), ii) in the presence of $2x10^{-4}$ M $MgCl_2$ (□), and iii) in the presence of $2x10^{-4}$ M $MgCl_2$ and 10^{-4} M sodium oleate (Δ). The dashed lines represent the constant charge model of the DLVO theory, whereas the solid line represents the extended DLVO theory (Eq. [5]) using the parameters shown in Table I. The arrows indicate the positions at which the two surfaces jump into contact

obtained here agrees well with the reported values in literature (12) for the Hamaker constant of the silica-water-silica system. The fact that ψ_o=0 mV under these conditions is not surprising. According to Fuerstenau *et al*. (5), the point of charge reversal (p.c.r.) of silica occurs at at pH≈10.5 at 10^{-4} M $MgCl_2$. Note that the force data obtained at $2x10^{-4}$ M $MgCl_2$ show no evidence for the hydration force. This is in sharp contrast to the observation made at pH 5.7, where the hydration force does not disappear in the presence of $2x10^{-4}$ M $MgCl_2$. Both the charge neutralization and the disappearance of the hydration force at pH 11.2 may be attributed to the adsorption of the $MgOH^+$ ions on the silica surface. As shown by the distribution diagram (dashed lines in Figure 4.3), the concentration of the $MgOH^+$ ions reaches maximum at pH 10.4.

In the presence of both $2x10^{-4}$ M $MgCl_2$ and 10^{-4}M sodium oleate at pH 11.2, the force data can be fitted ψ_o=-45 mV. Thus, oleate addition has rendered the surface more negative than at $2x10^{-4}$ M $MgCl_2$ alone, which can be attributed to the adsorption of the anionic surfactant. In the presence of oleate, the two surfaces jump into contact from a distance of H≈12 nm, which is substantially larger than predicted by the DLVO theory. This suggests the presence of a hydrophobic force. The solid line represents an extended DLVO fit to the data, where the hydrophobic force has been represented by the single exponential function (Eq.[1]) with C_o=-30 mN/m and D_o=2.1 nm. The presence of the hydrophobic force and increase in $-\psi_o$ strongly suggest that oleate adsorbs on silica at pH 11.2. It may be recalled that this is the same pH at which the silica surface is activated by $MgOH^+$ ions and the hydration force disappears.

Figure 4.4 shows three sets of force data obtained at pH 12, which include those obtained i) in water ii) in $2x10^{-4}$ M $MgCl_2$ solution, and iii) in a solution containing both $MgCl_2$ ($2x10^{-4}$ M) and sodium oleate (10^{-4} M). As can be seen, all the three sets of force data lie on the same curve. The parameters used to fit the data are given in Table I. The hydration force observed at this pH can be adequately represented by a single exponential function with a decay length of 0.42 nm. The short decay length may be attributed to the presence of the Na^+ ions added as NaOH to control pH. The fact that the force curves do not change in the presence of $MgCl_2$ and/or oleate suggest that neither of these species adsorb on silica at pH 12.2. This finding is in agreement with the fact that the values of θ_{eq} remain ~5^o.in the presence of $MgCl_2$ and oleate at this pH.

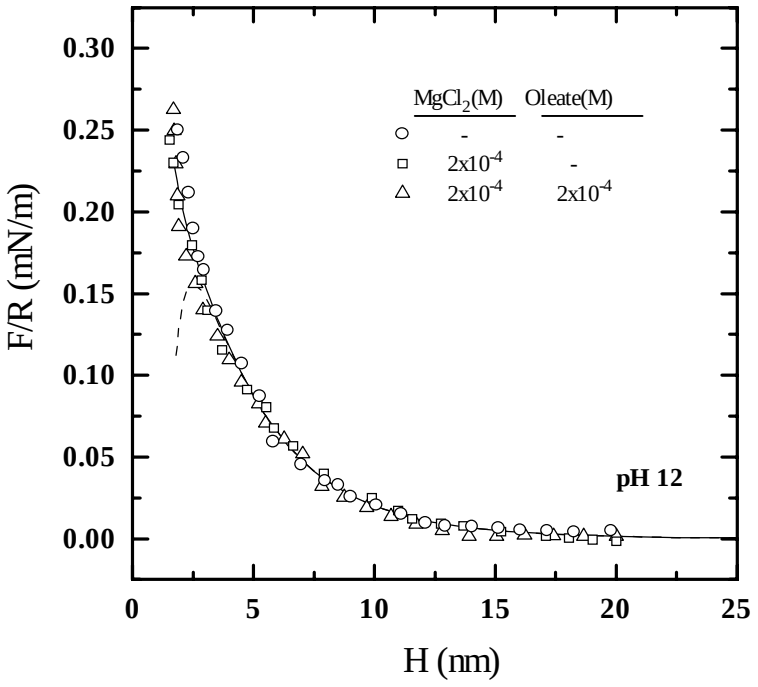

Figure 4.4. F/R vs H obtained between a silica plate and glass sphere at pH 12 in (i) absence of $MgCl_2$ and oleate (○), (ii) $2x10^{-4}$ M $MgCl_2$ (□) and (iii) $2x10^{-4}$ M $MgCl_2$ & 10^{-4} M Oleate (Δ). The dashed line represents the constant charge model of the DLVO theory whereas the solid lines represent the extended DLVO theory.

4.3b *Force Measurements with $CaCl_2$ and Oleate*

Figure 4.5 shows the values of θ_{eq} of silica plates in solutions containing both $2x10^{-4}$ M $CaCl_2$ and 10^{-4} M sodium oleate at various pHs. Shown by the dashed lines is the species distribution diagram at $2x10^{-4}$ M $CaCl_2$. The thermodynamic data used for the calculations were taken from reference 21. It can be seen from the Figure that at pH<11, where the concentration of $CaOH^+$ is low, silica remains hydrophilic with $\theta_{eq}=5^o$. At pHs>12, where $CaOH^+$ is present in significant quantities, the silica plate is rendered hydrophobic and exhibits $\theta_{eq}=65^o$. Contact angle measurements were not conducted at $pH>pH_{ppt}$. It has been reported (25), nevertheless, that silica is not effectively activated by Ca^{2+} ions if the ratio of Na^+ to Ca^{2+} ions in solution is greater than 10^3.

Force measurements were conducted for the $CaCl_2$-oleate-silica system at two different pHs: 5.7 and 12.2. Figure 4.6 shows the effect of $CaCl_2$ ($2x10^{-4}$ M) and sodium oleate (10^{-4} M) on the surface forces at pH 5.7. The figure also shows the force data obtained in the absence of $CaCl_2$ and oleate for comparison. It can be seen that $CaCl_2$ addition reduces both the long-range double layer repulsion and the short-range hydration repulsion. Table 4.2 shows the values of ψ_o, κ^{-1}, C_1, D_1, C_2 and D_2 obtained by fitting the data to the extended DLVO theory. The ψ_o and D_2 values obtained in the presence of $CaCl_2$ at pH 5.7 are very similar to those obtained in the presence of $MgCl_2$ at the same pH and concentration. Figure 4.6 and Table 4.2 show also that the force data obtained in a solution containing both $CaCl_2$ and oleate lie on the same curve as those obtained in the presence of $CaCl_2$ alone. This finding suggests that oleate does not adsorb on silica under these conditions.

Figure 4.7 shows the effect of $CaCl_2$ and sodium oleate at pH 12.2. Also shown for comparison are the force data obtained in the absence of $CaCl_2$ and oleate. The forces measured at H>3 nm are due to double layer repulsion and can be fitted to the DLVO theory with ψ_o=-11 mV and κ^{-1}=3.5 nm. The theoretical value of κ^{-1} at this pH is 2.8 nm, which compares very well with that obtained from fitting the force data. At H<3 nm, repulsive hydration forces are

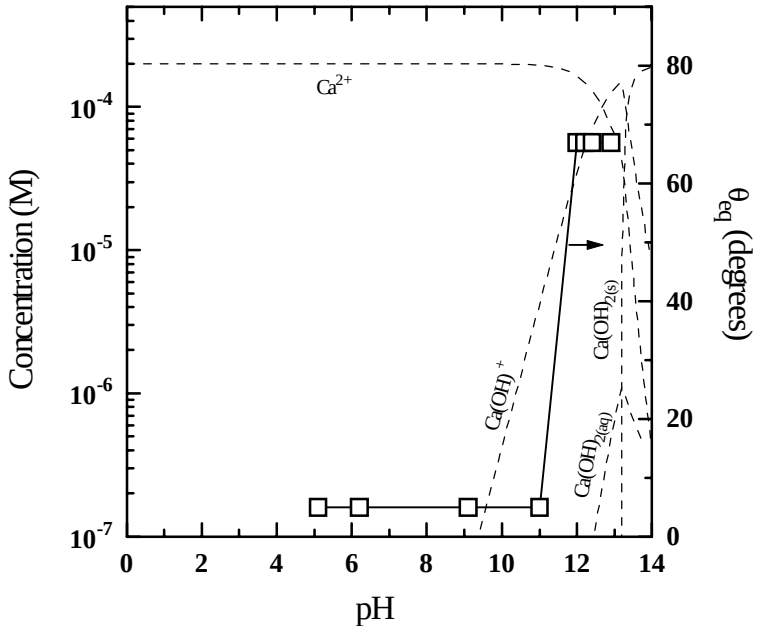

Figure 4.5. θ_{eq} vs pH curve (□) for a silica plate immersed at $2x10^{-4}$ M $CaCl_2$ and 10^{-4} M Na-Oleate. The dashed lines represent the solution concentrations of the various species in solution.

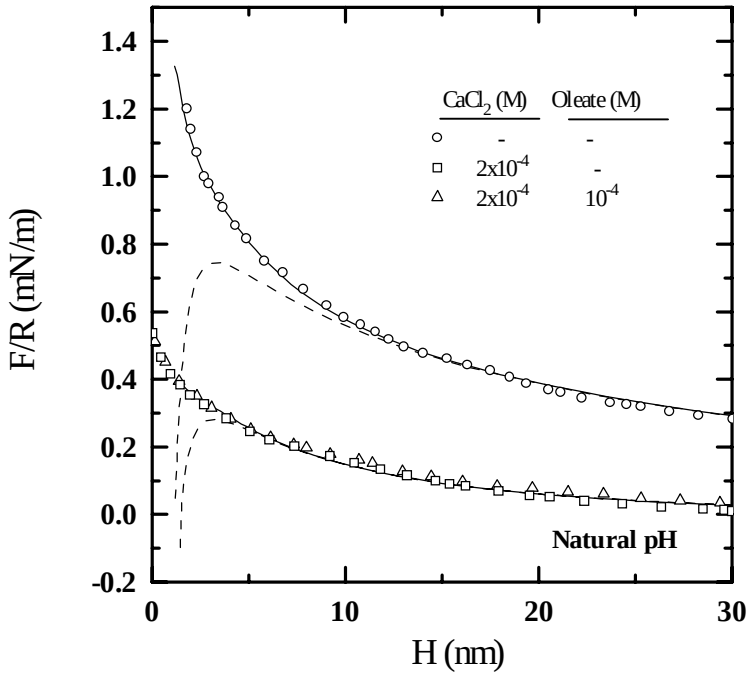

Figure 4.6. F/R vs H curves obtained between silica plate and glass sphere in i) Nanopure water (○), ii) at $2x10^{-4}$ M $CaCl_2$ (□), and iii) at $2x10^{-4}$ M $CaCl_2$ 10^{-4} M sodium oeate (Δ) at pH 5.7. The dashed lines represent the constant charge model of the DLVO theory and the solid lines represent the extended DLVO theory.

Table 4.2

Contact Angles and Parameters obtained from Fitting Force Curves between silica surfaces in solutions of $CaCl_2$ and Na-Oleate at different pHs

pH	$CaCl_2$ (M)	Oleate (M)	θ_{eq} (degrees)	ψ_0 (mV)	κ^{-1} (nm)	C_1 (mJ/m^2)	D_1 (nm)	C_2 (mJ/m^2)	D_2 (nm)
5.7	-	-	$<5^0$	-57	96.0	7.7	0.50	0.50	2.70
5.7	$2x10^{-4}$	-	$<5^o$	-18	15.0	7.6	0.44	0.37	1.25
5.7	$2x10^{-4}$	10^{-4}	$<5^o$	-18	15.0	7.6	0.44	0.37	1.25
12.2	-	-	$<5^o$	-11	3.5	8.0	0.45	-	-
12.2	$2x10^{-4}$	-	$<5^o$	+7	3.5	-	-	-	-
12.2	$2x10^{-4}$	10^{-4}	$<65^o$	-	-	-30.0	1.05	-	-

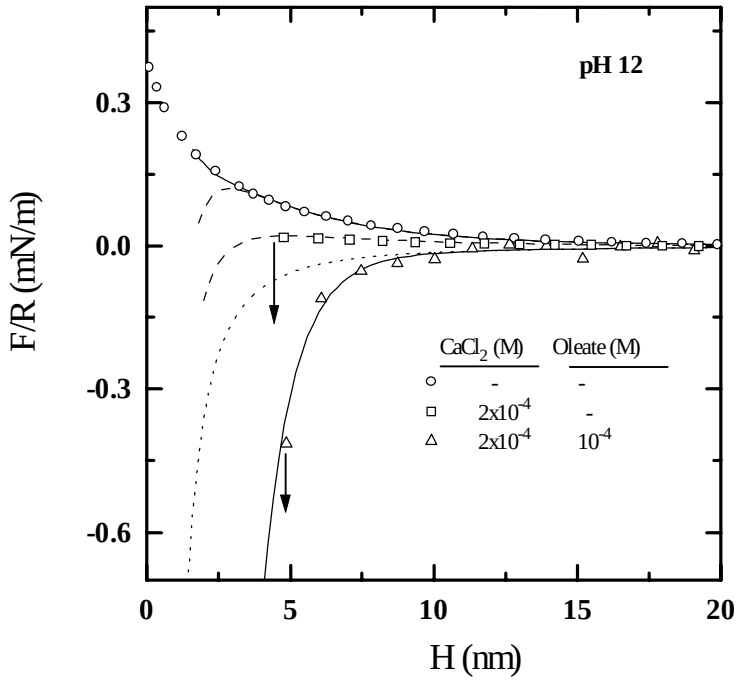

Figure 4.7. F/R vs H curves obtained between silica plate and glass sphere at pH 12.2 i) in Nanopure water (○), ii) at $2x10^{-4}$ M $CaCl_2$ (□), and iii) at $2x10^{-4}$ M $CaCl_2$ and 10^{-4} M sodium sleate (Δ). The dashed lines represent the constant charge model of the DLVO theory fitted to the force data. The solid line represents the extended DLVO theory (Eq. [5]) using the parameters shown in Table II. Also shown for comparison is the van der Waals force alone (dotted line).

.

observed, which can be fitted using the parameters shown in Table 4.2. Note that at $2x10^{-4}$ M $CaCl_2$, the magnitude of ψ_o is reduced to 7mV. Although the sign of ψ_o cannot be ascertained from force measurements, it is likely that the silica surface is positively charged under the conditions employed. Many investigators (9,12) have reported charge reversal of silica at pHs close to the pH_{ppt} of the hydrolizable cation. Note also that the two surfaces jump into contact at H=4 nm, and that there is no evidence of hydration repulsion. Since the concentration of $CaOH^+$ ions are high at pH 12.2, both the charge reversal and the disappearance of hydration force at this pH may be attributed to the specific adsorption of the singly charged hydroxo-complex on silica.

Also shown in figure 4.7 are the forces measured at $2x10^{-4}$ M $CaCl_2$ and 10^{-4} M Na-oleate at pH 12.2. No repulsive forces are observed at any separation distance. At H<10 nm, the experimental force data are more attractive than the van der Waals force, which indicates the presence of the hydrophobic force. The solid line represents the extended DLVO theory with the parameters shown in Table II. The D_2 value obtained here is lower than that obtained with $MgCl_2$ and oleate at pH 11.2. This is in agreement with the fact that the maximum θ_{eq} obtained for the $CaCl_2$-oleate-silica system is lower than that obtained for the $MgCl_2$-oleate-silica system. The results obtained in the presence of $CaCl_2$ suggest that oleate adsorbs on silica at pH 12.2 and renders the surface hydrophobic. The fact that hydrophobic force appears at the pH where the concentration of $CaOH^+$ ions is close to its maximum indicates that silica is activated by the singly charged hydroxo-complex.

4.4 Discussions

In the present work, hydrophobic forces have been observed for the first time between two negatively charged (silica) surfaces immersed in anionic surfactant (sodium oleate) solutions. To achieve this, it was necessary to activate the silica by reversing its surface charge, so that the anionic surfactant can adsorb on the surface and render it hydrophobic. Two hydrolizable cationic salts, $CaCl_2$ and $MgCl_2$, were used as activators. An important observation made in the present work was that strong hydrophobic forces were measured only at the pH values where the divalent

cations are hydrolyzed to form singly charged hydroxo-complexes, i.e., $CaOH^+$ and $MgOH^+$. This is evident from Figures 4.8 and 4.9, where the changes in the decay lengths (D_o of Eq. [1]) of the hydrophobic forces are plotted versus pH along with the species distribution diagrams at $2x10^{-4}$ M $MgCl_2$ and $CaCl_2$. Also shown in these two figures are the decay length (D_o or D_2 of Eq. [6]) of the hydration forces measured in $MgCl_2$ and $CaCl_2$ solutions as a function of pH. Interestingly, the hydration force disappears completely at the pH where the concentrations of $CaOH^+$ and $MgOH^+$ reach maximum. These findings suggest, therefore, that the singly charged hydroxo-complexes are the activating species, and that their adsorption on silica causes the hydration force to disappear and, at the same time, causes the anionic surfactant to adsorb and, hence, the hydrophobic force to appear.

The results obtained in the present communication may be compared with those of Pugh and Rutland (4), who conducted force measurements between mica surfaces in solutions of $CaCl_2$ and sodium laurate at pH 10.3. Unlike the silica surfaces used in the present work, the mica surfaces did not exhibit hydrophobic force, indicating that oleate did not adsorb on the surface. On the other hand, the authors observed disappearance of the 'secondary hydration force', which had been observed in the absence of $CaCl_2$. (Secondary hydration forces are observed when force measurements are conducted between mica surfaces in high concentrations of electrolytes (25,26).) The authors attributed the appearance of the hydration force to the presence of the Na^+ ions introduced to the system during pH adjustment, and its disappearance to the adsorption of $CaOH^+$ ions on mica. Displacement of the strongly hydrated Na^+ ions with the $CaOH^+$ ions from the mica surface should cause a decrease in hydration force, because the latter may be less strongly hydrated than the former owing to its large ionic size.

An interesting question to be raised here is why laurate/oleate ions adsorb on silica but not on mica despite the fact that $CaOH^+$ ions adsorb on both. Before embarking on the discussion, it should be noted here that the pH (=10.3) where Pugh and Rutland (4) conducted their force measurements with mica was considerably lower than the pH (=12.8) where the concentration of

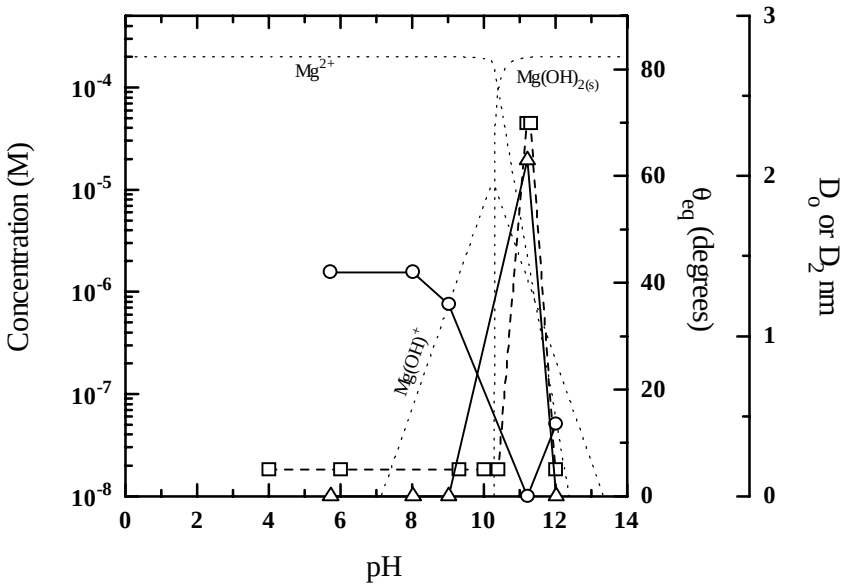

Figure 4.8. Effects of pH on D_o or D_2 of the hydration forces observed at $2x10^{-4}$ M $MgCl_2$ (○) and D_o of the hydrophobic forces observed at $2x10^{-4}$ M $MgCl_2$ and 10^{-4} M sodium oleate (Δ). The dashed lines represent the concentrations of the species present in solution. Also shown are the θ_{eq} (□) values.

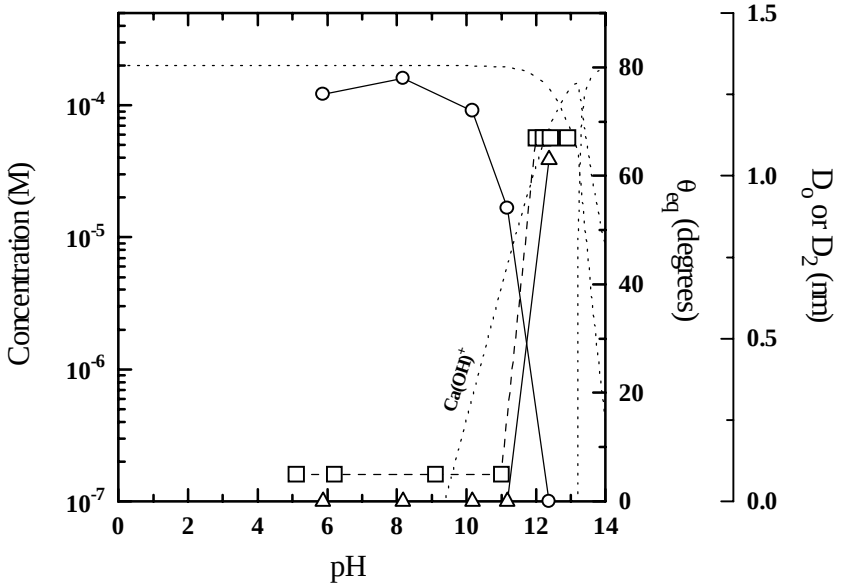

Figure 4.9. Effects of pH on D_o or D_2 of the hydration forces observed at $2x10^{-4}$M $CaCl_2$ (○) and D_o of the hydrophobic force at $2x10^{-4}$M $CaCl_2$ and 10^{-4}M oleate (Δ). The dashed lines represent the concentrations of the species in solution. Also shown are the θ_{eq} (□) values.

the $CaOH^+$ ions reaches maximum (see Figure 4.9.) Thus, it is possible that the low concentration of $CaOH^+$ ions at pH 10.3 is responsible for oleate not adsorbing on mica at this pH. To test this hypothesis, we measured water contact angles on mica with solutions containing $CaCl_2$ and oleate solutions in the pH range of 9.0-12.4. The results showed that the equilibrium contact angles (θ_{eq}) were in the range of 34-36^o and did not change with pH. These results show that oleate indeed does not adsorb on mica as suggested by Pugh and Rutland.

When sodium oleate is added to a solution containing calcium ions, a basic calcium oleate (CaOHOl) should form in solution at pH where the concentration of $CaOH^+$ ions is high enough to exceed its solubility limit. The basic calcium oleate cannot adsorb on the mica surface *via* a coulombic attraction as it is a neutral species. Nor is it possible for it to adsorb on the surface *via* chemical interaction or H-bonding mechanism, because the basal surface of mica consists of siloxane bonds and, therefore, is chemically inert. Silica, on the other hand, is capable of forming H-bonds with the CaOHOl species. Fuerstenau (28) suggested that the CaOHOl and MgOHOl species formed in solution adsorb on oxide surfaces *via* H-bonding.

The surface force measurements conducted in the present work show that silica is activated by $CaOH^+$ and $MgOH^+$ species rather than by Ca^{2+} and Mg^{2+} ions. Similar observations have also been made with other oxides using different techniques (5,8,29). In general, singly charged hydroxo-complexes adsorb on oxides in preference to unhydrolized divalent cations. Figure 4.10 shows an adsorption isotherm for Ca(II) species on silica as obtained by James and Healy (9). Dotted lines represent the concentrations of Ca^{2+} and $CaOH^+$ ions as a function of pH at 1.4×10^{-4} M Ca(II), which is the concentration at which the adsorption isotherm was established. As shown, the adsorption density increases with increasing concentration of $CaOH^+$ ions. No significant adsorption occurs at pH<9.0, where most of the Ca(II) species exist as Ca^{2+} ions.

The dashed line given in Figure 4.10 represents a theoretical isotherm derived from the James and Healy's model (Eq. [4]). It was obtained by calculating ΔG^o_{ads} from its three components, i.e., ΔG^o_{elec}, ΔG^o_{solv}, and ΔG^o_{chem}. Once the value of ΔG^o_{ads} is known, one can obtain

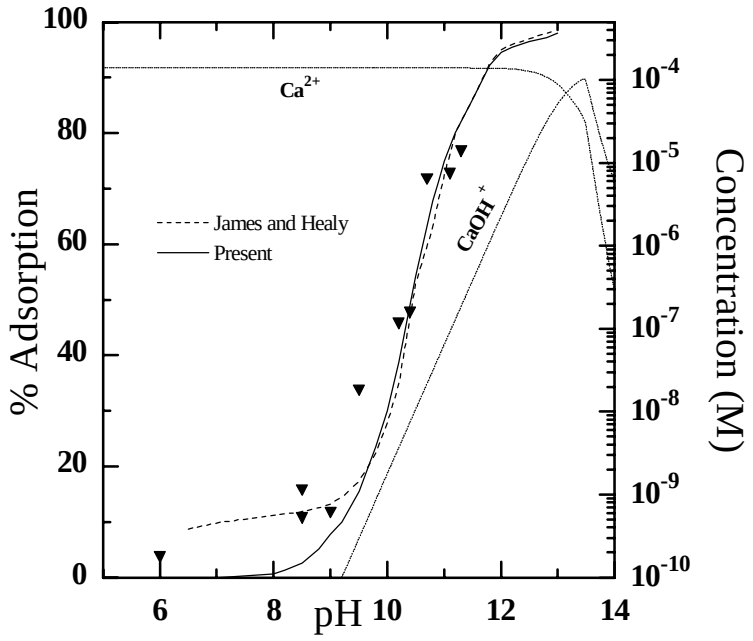

Figure 4.10. Adsorption of $CaCl_2$ (▼) as a function of pH, with the dashed line representing a theoretical fit using the James and Healy model (ref. 9). The solid line represents the model developed in the present work. The dotted lines represent the concentrations of Ca^{2+} and $CaOH^{+}$ ions at $2x10^{-4}$M $CaCl_2$.

.

the value of the equilibrium constant (K_i) of the adsorption equilibria using the following relationship:

$$K_i = \exp\left(-\Delta G^{o}_{ads}/RT\right) \tag{8}$$

where R is the universal gas constant and T is the absolute temperature. The adsorption equilibria were given by

$$(1-\Theta) + M_i \overset{K_i}{=} \theta_i \tag{9}$$

where M_i is the concentration of species i, θ_i the fractional surface coverage by species i, Θ is the fraction of the surface sites occupied by all adsorbates, i.e. $\Theta=\Sigma_i\theta_i$. Eq. [9] yields:

$$\Theta = \frac{\sum_i K_i M_i}{1+\sum_i K_i M_i} \tag{10}$$

which represents the theoretical adsorption isotherm of James and Healy given in Figure 4.10.

For ΔG^{o}_{elec}, James and Healy used the following relationship:

$$\Delta G^{o}_{elec} = -zF\psi_x \tag{11}$$

where z is the valence of the species under consideration, F the Faraday constant, and ψ_x is the potential at a distance of x away from the surface. The distance x used in this calculation was the sum of the radius of the adsorbing ion and the diameter of water (0.14 nm). Thus, the authors considered that ionic species adsorb on silica without losing the water molecules from the primary hydration sheath. It should be noted here that ψ_x is a function of surface potential (ψ_o), the values of which were obtained using the Nernst equation:

$$\psi_o = 2.3RT/zF\ (pH_{pzc}\text{-}pH) \tag{12}$$

where pH_{pzc} is the pH of pzc of silica. Finally, James and Healy fitted the theoretical isotherm to the experimental data using ΔG^{o}_{chem} as a fitting parameter. They obtained the value of -29.4 kJ/mole for both Ca^{2+} and $CaOH^{+}$ ions.

A problem associated with the James and Healy's model is that the values of ψ_o obtained using the Nernst equation were higher than those determined in the present work from direct surface force measurement by nearly an order of magnitude (see Figure 4.11). According to Hunter (30), Nernst equation should not be used in calculating ψ_o for oxides. It may be useful, therefore, to calculate ΔG^{o}_{elec} using the more realistic values of ψ_o. Also, it may be reasonable to consider ΔG^{o}_{sol} to be part of ΔG^{o}_{ads}. The reason is that dehydration is a prerequisite for chemisorption. Eq. [4] may then be reduced to:

$$\Delta G^{o}_{ads} = \Delta G^{o}_{elec} + \Delta G^{o}_{chem}. \qquad (13)$$

In the present work, the values of ΔG^{o}_{elec} were calculated using Eq. [11]. The values of ψ_o were obtained from the experimental data given in Figure 4.10. Note that ψ_o decreases with increasing pH. This may be attributed to both double layer compression (due to the Na^{+} ions added for pH adjustment) and neutralization of the SiO^{-} sites by Na^{+} ions to form SiONa (31).

The model based on Eqs. [8], [11] and [13] was then fitted to the James and Healy's experimental data given in Figure 4.10 using ΔG^{o}_{chem} as an adjustable parameter. In this calculation, the $CaOH^{+}$ ions were considered as the activating species. The value of ΔG^{o}_{chem} used to fit the experimental data was -42 kJ/mole at all pHs. Such a large value of ΔG^{o}_{chem} cannot be accounted for by the H-bonding mechanism discussed earlier for the adsorption of CaOHOl on silica. In general, the free energy changes associated with H-bonding are in the neighborhood of -10 kJ/mole (32). Therefore, there may be additional mechanism(s) involved in the activation of silica by $CaOH^{+}$ ions. Subtracting the free energy of adsorption due to H-bonding from the value of ΔG^{o}_{chem} obtained from the model, one obtains a value of -32 kJ/mole, which should be accounted for by additional mechanism(s). One possible mechanism may be the lateral interactions between adsorbed hydroxo- complexes on the substrate. Figure 4.12 depicts how

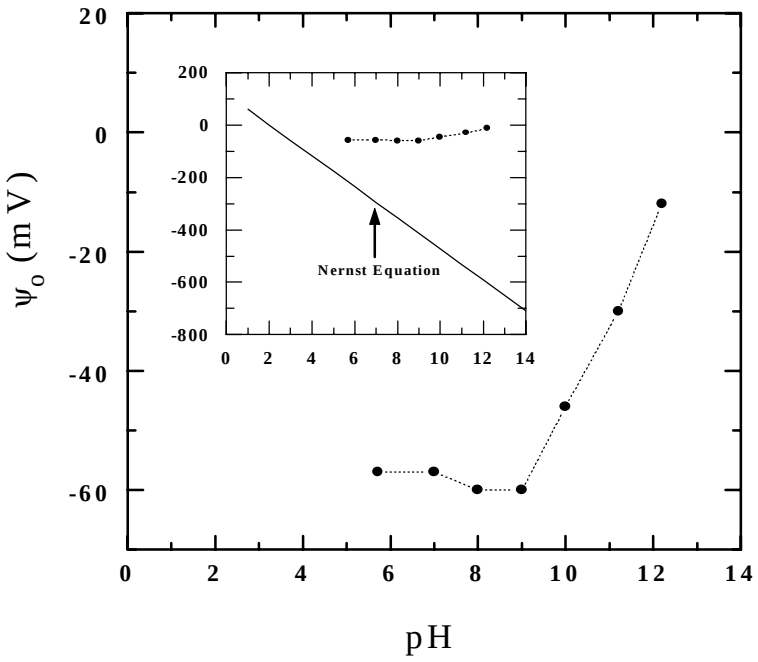

Figure 4.11. The values of ψ_o (●) obtained from the AFM force measurements. The inset compares the them with those obtained using the Nernst Equation.

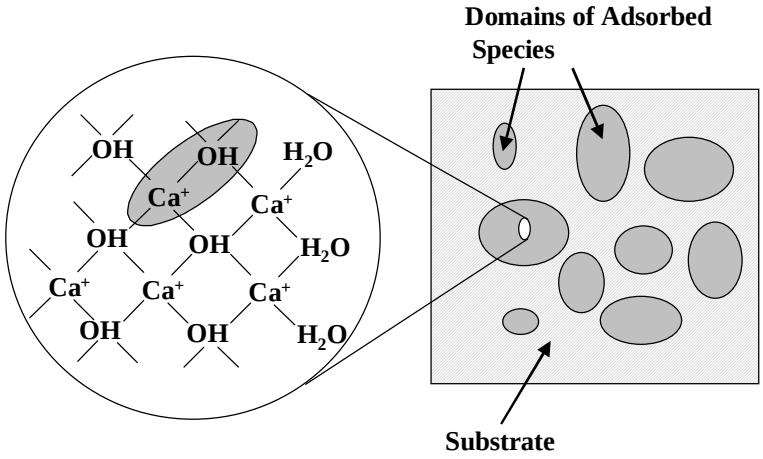

Figure 4.12. A conceptual model for the adsorption of $CaOH^+$ ions on a substrate. Domains (or clusters) of adsorbed species are formed due to lateral interactions.

.

$CaOH^+$ species may adsorb on silica surface by forming lateral bonds. Neighboring $CaOH^+$ species may interact with each other to form two-dimensional 'crystals', clusters or domains with free energy changes of -32 kJ/mole.

Thus, ΔG^o_{chem} may be considered to consist of two components, i.e.,

$$\Delta G^o_{chem} = \Delta G^{o,H}_{chem} + \Delta G^{o,l}_{chem} \quad (14)$$

where $\Delta G^{o,H}_{chem}$ is due to H-bonding with the silanol groups on the surface and $\Delta G^{o,l}_{chem}$ is due to the lateral interactions with neighboring adsorbates. $\Delta G^{o,l}_{chem}$ may be due to H-bonding or covalent bonding, the latter being more likely. For the $CaOH^+$ ions adsorbing on silica, $\Delta G^{o,l}_{chem}$=-32 kJ as discussed in the foregoing paragraph. This value is close to the free energy of the following reaction:

$$Ca(OH)_2(aq) = Ca(OH)_2(s) \quad (15)$$

whose ΔG^o is -30 kJ/mole (21). It is also close to the value of the following reaction:

$$4MgOH^+ = Mg_4(OH)_4^{4+} \quad (16)$$

whose ΔG^o is -34.3 kJ/mole (33). In both reactions [15] and [16], bulk of the free energy changes are due to covalent bonding. Therefore, $\Delta G^{o,l}_{chem}$ of -32 kJ for $CaOH^+$ ions adsorbing on silica is probably due to covalent bonding.

The adsorption model presented here is conceptually similar to the hemimicelle theory of Gaudin and Fuerstenau (34), who proposed that the specific adsorption of ionic surfactants may be due to the van der Waals interaction between adjacent hydrocarbon chains. Similarly, the adsorption of the singly-charged hydroxo-complexes may be favored due to the large value of -ΔG^o_{chem}, the major part of which seems to come from the lateral interaction between adsorbed hydroxo-complexes. This may provide an explanation for the observation that $CaOH^+$ and

$MgOH^+$ ions adsorb on silica but not Ca^{2+} and Mg^{2+} ions. Inability of the latter to adsorb on silica may also be attributed to the unfavorable electrical repulsion between adsorbed species.

An interesting observation made in the present work was that activated silica does not exhibit hydration force. One possible explanation would be that the surface of activated silica is less strongly hydrated than that of unactivated silica. This view may be supported by the fact that the standard free energy of hydration (ΔG^o_{hyd}) for Si^{4+} ions is -26,220 kJ/mole, while that of Ca^{2+} ion is -2,932 kJ/mole. These values were calculated from the formula (35): $\Delta G^o_{hyd} = -136.9z^2/r$, where z is the valence of the cation under consideration and r is its radius. The weakly hydrated surface may fail to support a strong H-bonded network of water molecules in the vicinity of silica, which is probably the origin of the primary hydration force observed with unactivated silica.

4.5 Conclusions

An atomic force microscope (AFM) was used to measure the surface forces between silica surfaces coated with self-assembled monolayers of sodium oleate. Since the surface charge of silica is of the same sign as the charge of oleate ions, it was necessary to reverse the charge of the silica substrate (which is a process referred to as "activation") by adding $CaCl_2$ or $MgCl_2$ to the solution. The results showed the presence of the long-range hydrophobic forces that have not been considered in the DLVO theory. The hydrophobic forces become strongest at the pH where the concentration of $CaOH^+$ or $MgOH^+$ ions reaches maximum. It is, therefore, suggested that calcium hydroxy-oleate (CaOHOl) and magnesium hydroxy-oleate (MgOHOl) adsorb on the silica surface possibly *via* H-bonding.

The force measurements were also conducted in $CaCl_2$ and $MgCl_2$ solutions in the absence of sodium oleate. The results showed that the primary hydration forces, which are observed in Nanopure water, disappear completely at the pH where the concentration of the $MgOH^+$ or $CaOH^+$ ions reaches maximum. This may be attributed to the fact that the silica surface is covered by the hydroxo-complexes that are not as strongly hydrated as the silanol groups on the surface of

silica. Thus, the AFM force measurements showed that the singly charged hydroxo-complexes are the activators.

A theoretical model was developed to better understand the mechanisms involved in the adsorption of the singly charged hydroxo-complexes on silica. In the present work, the free energy of adsorption (ΔG^{o}_{ad}) was back-calculated from the adsorption isotherm for the hydroxo-complexes on silica. From this, one can subtract the free energy of adsorption (ΔG^{o}_{elec}) due to electrostatic interaction, which can be readily calculated from the surface potentials (ψ_o) of silica determined from the AFM force measurements, to obtain the free energy of adsorption (ΔG^{o}_{chem}) due to chemical interaction. For the adsorption of $CaOH^+$ ions on silica, one obtains that ΔG^{o}_{chem}=-42 kcal/mole. By subtracting the value of H-bonding of the hydroxo-complex with the silanol groups on the surface, which may be estimated to be -10 kcal/mole, one obtains -32 kcal/mole. This value is close to the free energy of polymerization of $Ca(OH)_2$(aq) species, which is -30 kcal/mole. This finding suggests that the lateral interactions between neighboring adsorbates contribute most significantly to the adsorption of singly charged hydroxo-complexes on silica, followed by H-bonding with silanol groups and electrostatic interaction.

4.6 References

1. Israelachvili, J., and Pashley, R. M. *Nature* **300,** 341 (1982).
2. Herder, P. C., *J. Colloid Interface Sci.* **134,** 346 (1990).
3. Pashley, R. M., McGuiggan, P. M., Ninham, B. W. and Evans, D. F. *Science* **229,** 1088 (1985).
4. Pugh, R. J. and Rutland, M. *Proc. XX IMPC,* 583 (1997).
5. Fuerstenau, M. C., Elgillani, D. A. and Miller J. D. *Trans. AIME*, **247,** 11 (1970).
6. Fuerstenau, M. C. *AICHE Symposium Series.* **150,** 16 (1975)
7. Fuerstenau, M. C. and Cummins, W. F. *Trans. AIME,* **238,** 196 (1967).
8. Palmer, B. R., Gutierrez, G. B. and Fuerstenau, M. C. *Trans. AIME* **258,** 257 (1975).
9. James, R. O. and Healy, T. W. *J. Colloid Interface Sci*, **40,** no. 1, 65 (1972).
10. Schindler, P. W., Furst, B., Dick, R. and Wolf, P. U. *J. Colloid Interface Sci.* **55,** 469 (1976).
11. Ducker, W. A., Senden, T. J., and Pashley. R. M. *Nature* **353,** 239 (1993).
12. Grabbe, A. and Horn, R. G. *J. Colloid Interface Sci*. **157,** 375 (1993).
13. Yoon, R-H. and Subramanian, V. *J. Colloid Interface Sci.*, accepted for publication.
14. Peschel, G., Belouschek, P., Muller, M. M., Muller, R. M., and Konig, R. *Colloid Polymer Sci*. **260,** 444 (1982).
15. Yotsumoto, H., and Yoon, R-H. *J. Colloid Interface Sci.* **157,** 434 (1993).
16. Chapel, J.*Langmuir*, **10**, 4237 (1994).
17. Meagher, L. *J. Colloid Interface Sci.***152,** No.1, 293 (1992)
18. Rabinovich, Ya. I., Derjaguin, B. V. and Churaev, N. V. *Adv. Colloid Interface Sci.* **16,** 63 (1982).
19. Senden, T. J. and Ducker, W. A. *Langmuir* **10,** 1003 (1994).
20. Rabinovich, Ya. I. and Yoon, R.-H. *Colloids and Surfaces,* **93,** 263 (1994).
21. *Standard Potentials in Aqueous Solutions* (A.J. Bard, R. Parsons and J. Jordan, Eds.), IUPAC, Marcel Dekker, Inc., New York (1985).
22. Derjaguin, B. V., and Landau, L. *USSR Acta Physicochim*. **14**, 633 (1941).
23. Verwey, E. J., and Overbeek, J. Th. G. *Theory of the Stability of Lyophobic Colloids* Elsiever, New York, 1947.
24. Chan, D. Y. C., Pashley, R. M., and White, L. R. *J. Colloid Interface Sci.* **77,** 283 (1980).

25. Cooke, S. R. B. and Digre, M. *AIME Trans.* **232,** 24 (1965).
26. Pashley, R. M. *J. Colloid Interface Sci.* **83,** 531 (1981).
27. Yotsumoto, H. and Yoon, R. H. *J. Colloid Interface Sci.* **157,** 426 (1993).
28. Fuerstenau, M.C. and Elgillani, D. A. *Trans. AIME* **235,** 405 (1966).
29. Fuerstenau, M.C., Rice, D. A., Somasundaran, P. and Fuerstenau, D. W. *Bull. Inst. Min. and Met, London.* **701,** 381 (1965).
30. Hunter, R. J. *Foundations of Colloid Science,* Calrendon Press, New York (1987).
31. Allen, L. H. and Matijevic, E. J. *Colloid and Interface Sci.* **31,** 287 (1969).
32. Vinnagradov, S. N. and Linnell, R. H. *Hydrogen Bonding*, Van Nostrand Reinhold Co. (1971).
33. Baes, C. F. and Mesmer, R. E. *The Hydrolysis of Cations*, John Wiley and Sons, Inc., 1976.
34. Gaudin, A. M. and Fuerstenau, D. W. *Trans. AIME* **202,** 958 (1955
35. Harvey, K. B. and Porter, G. B. *Introduction to Physical Inorganic Chemistry*, Addison-Wesley Publishing Co., Inc., 1963.